

Water mass structure defines the diapausing copepod distribution in a right whale habitat on the Scotian Shelf

Kimberley T. A. Davies^{1,*}, Christopher T. Taggart¹, R. Kent Smedbol^{1,2}

¹Department of Oceanography, Dalhousie University, 1355 Oxford St., Halifax, Nova Scotia, B3H 4R2, Canada

²Fisheries and Oceans Canada, Bedford Institute of Oceanography, 1 Challenger Drive, Dartmouth, Nova Scotia, B2Y 4A2, Canada

ABSTRACT: North Atlantic right whales *Eubalaena glacialis* aggregate in Roseway Basin on the western Scotian Shelf where their energy-rich food sources, diapausing copepods *Calanus* spp., are concentrated at depth. The Canadian Species at Risk Recovery Strategy for right whales provides provisional Critical Habitat (CH) boundaries for Roseway Basin based on right whale occupancy, with the stipulation that the boundaries be refined using spatially explicit indicators of CH, specifically the environmental, oceanographic, and bathymetric conditions responsible for the copepod aggregations and distribution. We measured the concentration, energy density, spatial distribution, and extent of the right whale food base and the related oceanography at depth in the Basin during late-summer 2008 with the goal of refining the spatial extent of right whale CH. We show that the diapausing copepods were distributed throughout the Basin, with elevated concentrations located at depth toward the northeast and along the southern Basin margin slope. The aggregations were associated with warm, salty, high-density (26.0 to $26.2 \sigma_t$ kg m^{-3}), continental slope-influenced water masses and not with cold, fresh, low-density ($<26.0 \sigma_t$) water masses originating on the Scotian Shelf. Tidally driven variation in the copepod aggregations across the southern slope was coincident with the movement of the $26.0 \sigma_t$ isopycnal. We propose a mechanism, based on water mass density and advection, that explains the spatial and temporal (e.g. inter-annual) variation in diapausing *Calanus* energy density (joules per unit ocean volume) distribution, and by proxy, variation in right whale occupancy of the Basin. We further propose that the provisional CH boundaries, partly conditioned on vessel-strike mitigation measures, be extended to better encompass the critical feeding habitat. This could be achieved without compromise regarding vessel traffic and existing vessel-strike mitigation.

KEY WORDS: North Atlantic right whale · Critical Habitat · Roseway Basin · Water mass density · Slope water · *Calanus finmarchicus* · *Calanus hyperboreus* · Conservation

—Resale or republication not permitted without written consent of the publisher—

INTRODUCTION

North Atlantic right whale Critical Habitat

North Atlantic right whales *Eubalaena glacialis* (hereafter right whales) are an Endangered species that migrates to Canadian maritime waters to feed in summer (June through October). Grand Manan Basin in the Bay of Fundy and Roseway Basin on the

Scotian Shelf are primary areas of right whale aggregation, and the pioneering work of Murison & Gaskin (1989) identified Grand Manan Basin as a likely feeding habitat. The 2 basins were initially designated, but not legislated, as Right Whale Conservation Areas in 1993, and subsequent research focused on discerning the relationship between right whales and their food. Effort initially focused on the Grand Manan Basin due to the consistent annual occupancy

*Corresponding author: kim.davies@dal.ca

by right whales. Roseway Basin was considered a more ephemeral habitat due to high variation in right whale occupancy (Kraus & Rolland 2007). Research in Grand Manan Basin confirmed that right whales feed on deep, diapausing layers of the copepod *Calanus finmarchicus* stage-C5 (Woodley & Gaskin 1996, Baumgartner & Mate 2003, Baumgartner et al. 2003a,b). Thereafter, the temporal and spatial extent of the deep copepod layer measured by Michaud & Taggart (2007, 2011) was used to help delineate the boundaries of the now-defined Critical Habitat (CH) in Grand Manan Basin as required under the Canadian Species At Risk Act (SARA) and the right whale Recovery Strategy (Brown et al. 2009). The Recovery Strategy defines CH as 'areas that possess the environmental, oceanographic and bathymetric conditions that aggregate concentrations of right whale prey, especially stage-C5 *Calanus finmarchicus* copepodites, at interannually predictable locations' (Brown et al. 2009, p. 28).

Roseway Basin (Fig. 1) is also a habitat where right whales recurrently aggregate (Baumgartner & Mate 2003, 2005, Kraus & Rolland 2007, Vanderlaan et al. 2008) and where diapausing *Calanus finmarchicus* stage-C5 and *C. hyperboreus* stage-C4 are abundant (Baumgartner et al. 2003a, Davies et al. 2013). Unlike Grand Manan Basin, no spatially explicit surveys of the right whale prey field have been conducted in Roseway that could help define CH in the SARA Recovery Strategy. Thus, the Recovery Strategy contained provisional CH boundaries based on the historical spatial probability distribution of the whales (Vanderlaan et al. 2008) with the stipulation that the boundaries be refined upon collection of spatially explicit habitat indicators (Brown et al. 2009). The data presented in this manuscript were collected, in part, to refine the boundaries for the above right whale conservation purposes. Thus, our overall aim was to measure the concentration, energy density, spatial distribution, and extent of the right whale food base in Roseway Basin, and to do so in relation to the local oceanography, with the ultimate goal of refining the right whale CH in the Roseway Basin area.

Variation in right whale distributions and habitat

More than half of the only known northern right whale population is distributed in spring and summer among 5 known CHs in the Gulf of Maine, the Bay of Fundy, and the western Scotian Shelf regions (Kraus & Rolland 2007). The latter region lies near the south-

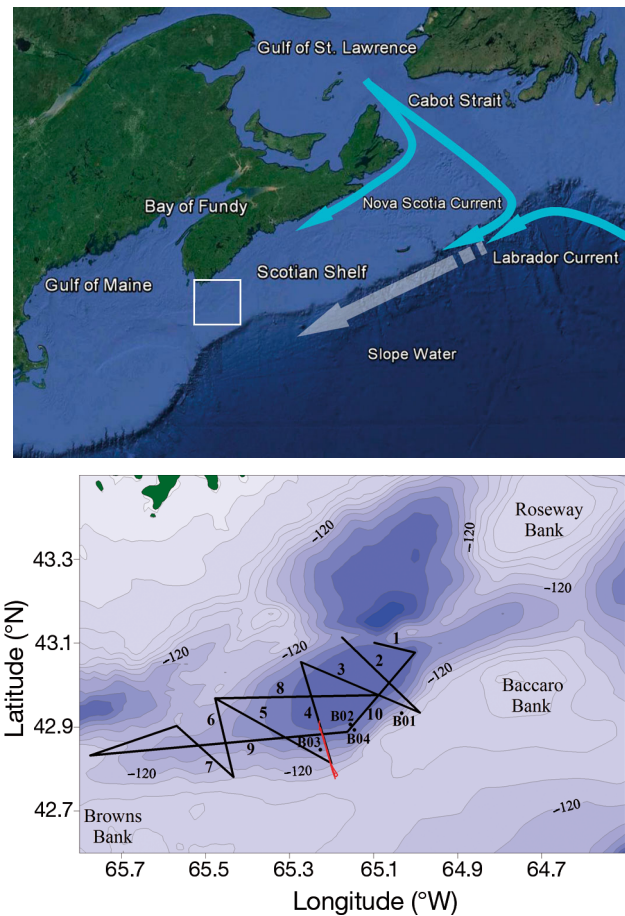


Fig. 1. The Scotian Shelf and surrounding regions, showing general circulation features with a bathymetric (10 m interval) chart (inset) of Roseway Basin and the 2008 survey showing the TUBSS survey transects (1–10, solid black lines), the 24 h tidal transect (solid red line), and the 4 BIONESS sampling locations (B01 to B04; solid black circles)

ern extent of the *Calanus* geographic range (Fleminger & Hulsemann 1977, Planque & Batten 2000) and near the northern extent of the known contemporary right whale migratory distribution (Kraus & Rolland 2007). Of the 5 habitats, Roseway Basin is considered the most ephemeral. The number of right whales annually observed in the Basin is highly variable, ranging from 0 to 117 (Vanderlaan 2010), and this variation is postulated to result from variation in food availability (Patrician & Kenney 2010). This degree of variation provides an opportunity to determine not only the limits of the 'critical habitat' but the opportunity to explain the prey field variation within the habitat that presumably influences variation in right whale occupancy.

Right whales require highly concentrated food (e.g. at least 7 kJ m^{-3} , Kenney et al. 1986) within a feeding

habitat to maximize their energy intake and must therefore rely on biophysical processes that aggregate their prey (Kenney et al. 1986, Baumgartner et al. 2007). Thus, variability in the environmental conditions that affect *Calanus* aggregations is thought to explain variation in right whale habitat use (Kenney et al. 2001, Baumgartner et al. 2003a, Baumgartner & Mate 2003). Two ways in which *Calanus* aggregations can vary in time and space are through the advection of *Calanus*-rich source waters into the CHs, which affects basin-scale concentrations (Head et al. 1999), and through physical oceanographic mechanisms that aggregate the copepods in high concentration at the scale of a foraging animal (Baumgartner et al. 2003b, Michaud & Taggart 2011, Davies et al. 2013). Each of these processes is considered below.

Local-scale *Calanus* aggregations

An observer in Roseway Basin has the highest probability of sighting a right whale along the southern margin of the Basin, just north of the 100 m isobath (Vanderlaan et al. 2008). Under the hypothesis that the probability distribution of whales reflects the distribution of their food, we undertook a study near the Basin margin to investigate the mechanisms that contribute to the margin being a *Calanus* aggregation area (Davies et al. 2013). The study demonstrated that the diapausing copepods were highly concentrated at depth along the southern slope of the Basin below the 26 σ_t (kg m^{-3}) isopycnal where they were advected by the cross-isobath tidal current that converged on the slope, and by an along-isobath sub-tidal flow. As in Michaud & Taggart (2011), an accumulation mechanism was postulated whereby the copepods are advected above their isopycnal of neutral buoyancy ($\sim 26 \sigma_t$) by vertical currents, then sink back to this density layer, in a vertically sheared horizontal tidal current. The measurements and mechanisms reported by Davies et al. (2013) were based on geographically fixed physical and biological observations over time (i.e. a time series) and thus left the following questions unanswered: (1) Does the hypothesized mechanism create predictable accumulation zones of whale food on the slope at tidal frequencies? (2) Are the diapausing copepod concentrations on the slope elevated compared to the rest of Roseway Basin, or are there alternative reasons why the slope may be a favorable feeding area? (3) Are there other areas in the Basin that have the environmental characteristics favorable for right whale feeding? (4) Are the diapausing copepods concentrated

near and (or) below the 26 σ_t isopycnal throughout the Basin, or is this characteristic unique to the southern slope? (5) How do the answers to these questions relate to the definition of CH?

Calanus source-water advection into Roseway Basin

In general, water mass structure and circulation on the Scotian Shelf (Fig. 1) is primarily influenced by (1) variation in seasonal air–sea interactions, (2) waters originating from the Gulf of St Lawrence (GoSL) through the Cabot Strait, from the Newfoundland Shelf via the Labrador Current, and from offshore continental slope water, and (3) tidal mixing in the Gulf of Maine (Han et al. 1997, Hannah et al. 2001). It is well established that the Scotian Shelf has 2 major water masses that advect *Calanus* spp. to the deep Shelf basins (Tremblay & Roff 1983, Sameoto & Herman 1990, Herman et al. 1991, Head et al. 1999, McLaren et al. 2001, Zakardjian et al. 2003). The first is a cold, freshwater mass originating in the GoSL that contains cold-adapted (Arctic) *C. glacialis* and *C. hyperboreus*, as well as the boreal *C. finmarchicus*, and is transported SW along the inner Shelf by the Nova Scotia Coastal Current (NSCC). The second is the warm and salty slope water that contains high concentrations of *C. finmarchicus*. The outer arm of the GoSL water flows south along the eastern margin of the Scotian Shelf and then SW along the continental slope where it mixes with slope water before intruding on-shelf into the central and western Shelf basins. As a consequence, the basins on the eastern Scotian Shelf (e.g. Louisbourg Basin) are dominated by cold-adapted copepods, whereas basins on the central and western Scotian Shelf are dominated by *C. finmarchicus*. It is hypothesized that the addition of slope water to the central and western Scotian Shelf plays a pivotal role in the population dynamics of *C. finmarchicus* on the Shelf (Head et al. 1999, Zakardjian et al. 2003), and that inter-annual variation in slope-water intrusions to Roseway Basin may explain variation in *C. finmarchicus* and right whale abundance in the Basin (Patrician & Kenney 2010). Hence, we asked a second set of questions: (1) Does the spatial distribution of *Calanus* within Roseway Basin reflect the spatial distribution of slope-influenced water in the Basin? (2) Is this related to the spatial distribution of the 26 σ_t isopycnal, as was found on the southern slope region of the Basin (Davies et al. 2013)? The answers to these questions should provide the environmental determinants of right whale CH in Roseway Basin.

Objectives

To answer the above sets of questions, our first objective was to measure the concentration (m^{-3}), energy density (kJ m^{-3}), spatial distribution, and extent of the right whale prey field (*Calanus*) in Roseway Basin. Our second objective was to examine the oceanographic and bathymetric conditions responsible for the Basin-scale accumulation of diapausing *Calanus*. Specifically, we address the 5 questions above that stemmed from the study by Davies et al. (2013) on the southern Basin margin. We then addressed the remaining 2 questions by examining the Basin-scale relationships among *Calanus* concentration, slope-influenced water, and the depth of the 26 σ_t isopycnal. We accomplished our objectives by simultaneously measuring the spatial distribution of *Calanus* and the hydrography using an optical plankton counter and CTD platform towed along- and across-Basin transects, with a concentrated effort on the southern margin during a 24 h period (2 tidal cycles). We used the results to redefine the right whale CH for Roseway Basin, and evaluated the veracity of the provisional CH boundaries.

MATERIALS AND METHODS

Biological and hydrographic data collection

An oceanographic survey aboard the RV 'Dominion Victory' was conducted in Roseway Basin during 4 through 13 September 2008 (Fig. 1). Zooplankton samples were collected at 4 stations using a Bedford Institute of Oceanography Net and Environmental Sampling System (BIONESS; Sameoto et al. 1980) towed at a nominal 1 m s^{-1} and equipped with 5 to 7 nets (333 μm mesh, 1 m^2 opening, 1.5 m length). The BIONESS was initially fitted with a Seabird-19 CTD (Seabird Electronics) and 2 G.O. flow meters (General Oceanics) to estimate filtered volume (real-time data) and an optical plankton counter (OPC-1T, Focal Technologies; Herman 1988, 1992) that also provided real-time data. A data stream failure from the Seabird-19 CTD and the flow meters required us to use a Seabird-37 microCAT CTD (archival data). Thus, the flow estimates for the net tows and the OPC were calculated using speed over ground recorded by vessel GPS and the change in depth recorded by the CTD. As BIONESS data were also collected in the Basin in 2009 with functional flow meters, we used those data to calibrate our 2008 flow estimates. At stations B01, B03, and B04, BIONESS Net-1 collected

a sample from the surface to ~10 m above bottom while subsequent nets sequentially opened and closed to sample discrete depth strata between near bottom and the surface. At station B02, the BIONESS tow was completed with all nets opening and closing within the 130–160 m depth stratum to estimate small-scale spatial variation in the prey field at depth. Once recovered, each net collection was filtered through a 330 μm sieve and preserved in 4% buffered formalin.

Zooplankton taxonomic, size frequency, and energy content analyses

All large and rare organisms (macrozooplankton; nominally $>2 \text{ cm}$) were sorted from the formalin-preserved net collections, identified to family, and counted. The remainder of each sample (mesozooplankton; nominally 333 μm to 1 cm) was partitioned using a Folsom splitter until replicate sub-samples of 150 to 200 copepods were obtained. All zooplankton in each sub-sample were counted and identified: copepodids to genus, species, and stage and the others to the highest taxonomic resolution possible. Sequential replicate sub-samples were examined until the coefficient of variation (CV) for both the dominant copepod species and stage and the total number of copepods either decreased to ~10% or less, or stabilized, or until a maximum of 6 sub-samples had been examined. Generally 3 to 4 replicates were required and the average CV for the total number of copepods and C5s consistently ranged between 10 and 11%. The concentration (m^{-3}) of each species collected in each BIONESS net is presented in Supplementary Tables S2 to S5 of Davies et al. (2013). Random subsamples of 20 to 100 individuals of *Calanus finmarchicus* C5s (hereafter CF5) and *C. hyperboreus* C4s (hereafter CH4) from each net collection were photographed under a dissecting scope, and their length and width measured using Image-J (v. 1.41, <http://rsbweb.nih.gov/ij/>). The size distributions were used to sort the CF5s and CH4s into size classes (S_{net}) chosen to correspond with OPC digital bin classes (S_{opc}) that encompassed the observed S_{net} size frequency distribution.

Gross energy content (caloric, J) of individuals in each CF5 and CH4 size class was measured using a Parr® 1266 semi-micro oxygen-bomb calorimeter (complete details provided by Michaud & Taggart, 2007, 2011, Davies et al. 2012). This enabled us to apply size-specific energy terms to the copepod abundance-at-size distributions measured by the

OPC and thus energy density (J m^{-3} ; detailed below). The 4 CF5 digital bin-classes 8–11, measured as equivalent spherical diameter (ESD) in μm , ranged from 823–936, 943–1058, 1064–1182, and 1187–1307 μm ESD, respectively. The 3 CH4 digital bin-classes 11–13 ranged from 1187–1307, 1312–1434, and 1439–1562 μm ESD, respectively. As there is no difference in size-specific energy content between CF5s and CH4s (Davies et al. 2012), the data from bin-class 11, where the 2 species overlapped in size, were combined and thus the size class-specific energy content estimates were bin-class 8, 3.89 J; class 9, 5.71 J; class 10, 8.07 J; class 11, 9.31 J; class 12, 10.78 J; and class 13, 12.20 J, as in Davies et al. (2012).

TUBSS-OPC data collection and analysis

Zooplankton abundance-at-size estimates, particularly for the CF5 and CH4 combined size distribution, were obtained using an OPC attached to an Endeco V-fin along with a digital flowmeter and a Seabird-37 microCAT CTD. This Towed Underwater Biological Sampling System (TUBSS, Taggart et al. 1996, Sprules et al. 1998) was deployed in an undulating ('tow-yo') fashion between 50 m depth and ~10 m above bottom using a nominal vertical speed of 1 m s^{-1} and nominal vessel speed of 3 knots along a series of transects (Table 1, Fig. 1). Seven cross-Basin transects (Tr-1 to Tr-7), each 15 to 30 km in length, ran in a generally NW to SE zigzag pattern. Tr-8 was ~35 km in length and intersected Tr-4 and Tr-5. Two along-Basin transects (Tr-9, Tr-10) intersected the 7 cross-Basin transects. The SE half of Tr-4 was also transited 11 times over a 24 h period between 19:15 h on

11 September and 18:45 h on 12 September to capture tidal variation in zooplankton concentration and temperature across the southern margin of the Basin. The tidal transect orientation paralleled the long axis of the tidal ellipse that is oriented cross-slope (see Fig. 1c in Davies et al. 2013) and allowed estimates of tidally driven cross-slope variation in the prey field. Due to operator error, salinity and thus density data were only available for 2 of the 11 transits.

The OPC recorded plankton abundance-at-size data at 2 Hz. A non-functional CTD hardwired to the TUBSS platform prevented recording of pitch and flow meter data, and the CTD was replaced with the microCAT CTD that recorded data at 20 or 6 s intervals that were uploaded after each tow. Vessel GPS data were recorded at 60 s intervals. In lieu of flow meter data, tow speed was estimated as described above for BIONESS, and volume filtered was determined using the product of tow speed, elapsed time, and cross-sectional area of the OPC aperture. All data were interpolated, where needed, to 1 Hz records.

The majority of TUBSS-OPC data analyses follow Michaud & Taggart (2011). In summary, the plankton particles were classified by the OPC in 4096 digital bin-classes (DS_{opc}), each proportional to particle area. The particle equivalent spherical diameters (ESD_{opc} , μm) were then calculated from DS_{opc} using the following empirical equation (Taggart et al. 1996):

$$\text{ESD}_{\text{opc}} = 10^{0.575 \log[(\text{DS}_{\text{opc}}) + 1.870]} \quad (1)$$

To simplify the analysis, the number of digital bin-classes was reduced to 64 by using the integer value of $\text{DS}_{\text{opc}}^{1/2}$. Each ESD_{opc} measurement was placed

Table 1. Summary of each transect (numbered as in Fig. 1) in Roseway Basin during 5 to 14 September 2008, providing start and end dates (given as mm/dd) and times (h:min), latitude (lat, °N) and longitude (lon, °W), nominal heading, length (km), and maximum sampling depth (m)

Transect no.	Start date	Start time	End date	End time	Start lat	Start lon	End lat	End lon	Heading	Length	Max depth
1	09/06	01:31	09/06	03:10	43.077	65.002	43.100	65.097	NW	8.27	161
2	09/11	12:39	09/11	17:01	42.922	64.977	43.112	65.174	NW	27.00	163
3	09/11	07:44	09/11	12:03	43.074	65.278	42.930	64.982	SE	29.90	160
4	09/09	17:17	09/09	21:06	42.814	65.201	43.038	65.268	NW	26.17	161
5	09/13	20:11	09/13	17:37	42.967	65.480	42.875	65.315	SE	17.00	144
5	09/09	15:22	09/09	17:17	42.875	65.318	42.814	65.201	SE	12.08	143
6	09/08	22:10	09/09	01:50	42.960	65.477	42.780	65.433	SE	21.09	132
7	09/09	01:50	09/09	04:47	42.780	65.433	42.903	65.568	NW	17.89	128
8	09/13	20:11	09/14	00:45	42.967	65.480	42.976	65.089	E	31.88	161
9	09/05	21:00	09/06	01:30	42.898	65.164	43.076	65.002	NE	28.25	156
10	09/09	07:43	09/09	15:21	42.832	65.775	42.875	65.320	E	24.16	143
10	09/13	15:30	09/13	17:39	42.889	65.154	42.876	65.316	W	23.99	153

into 1 of the 64 bin classes, denoted by S_{opc} . The number of particles in each S_{opc} bin class was then recalculated at 1 Hz. *Calanus* concentration was estimated at 1 Hz by summing the S_{opc} bin classes that corresponded to the S_{net} size distribution (S_{opc} classes 9 through 16; see the Supplement at www.int-res.com/articles/suppl/m497p069_supp.pdf) and dividing by the sampled volume. *Calanus* concentration in each size class was then multiplied by the size-class-specific energy content (J), and the resulting energy density (kJ m^{-3}) series was integrated over all *Calanus* size classes. Energy terms were measured for copepods in S_{net} classes 8 to 13. However, the OPC-measured copepods concentrated in S_{net} classes 7 to 14, so we assumed that energy content of copepods in class S_{net} 7 = class S_{net} 8, and class S_{net} 14 = class S_{net} 13. If invalid, the assumption had limited effect on estimates as very few of the copepods (tails of the size distribution) were assigned to S_{net} class 7 (mean ESD = 761 μm) or S_{net} 14 (mean ESD = 1630 μm ; see the Supplement). Finally, the TUBSS-OPC *Calanus* energy density estimates were calculated using the calibration based on the BIONESS-net and BIONESS-OPC energy density calibration (see the Supplement, particularly Fig. S3, for details).

The OPC-derived series of *Calanus* energy density was smoothed using a centered, uniformly weighted moving average with a 5 s window and again using a 7 s window. Water column sectional-profiles of hydrographic data and *Calanus* energy density were contoured using Surfer (Ver. 8, Golden Software) with gridding based on inverse square distance. The search ellipse radii for energy density estimates were 5 m vertical and 1.5 km horizontal. For hydrographic properties, the search ellipse radii were 10 m vertical and 3 km horizontal. The greater search radii were necessary for the hydrographic data as they were collected at lower resolution.

Planar (horizontal) distributions of the energy density estimates and hydrographic data, at depth, were estimated using the transect data whereby the estimates at each grid node (~ 5 m vertical resolution) were first integrated over each of the 100–120, 120–140, and 140–160 m depth strata as follows:

$$X = \sum \frac{x_i + x_j}{2} (z_i - z_j) \quad (2)$$

where X is the integrated value of the variable x over the lower (i) and upper (j) limits of each stratum z . The energy density estimates were expressed volumetrically (kJ m^{-3}) by dividing the X estimates by the thickness of the stratum. Subsets of the transect data

were 'advected' from their different times and geographic locations to a common time (high tide) using a numerical circulation model (WebDrogue Drift Prediction Model Ver. 0.66) as in Michaud & Taggart (2011). However, as the effect on the energy density field was well within the bounds of uncertainty, due to the small tidal excursion (3 km) relative to the extent of the prey field estimates ($\sim 45 \times 25$ km), and the horizontal data resolution (1.5 km), the advection of transect data to a common time was abandoned. The planar data were also contoured using inverse square distance using search ellipse radii of 0.06° N and 0.06° W.

RESULTS

Water masses in Roseway Basin

The water mass structure in the deeper (50–160 m) regions of Roseway Basin (Fig. 2) reflected a 3 end-member system (i.e. 3 different water masses of different origin, as defined by their temperature and salinity characteristics, that are mixed in varying proportions depending on location in the Basin), where the end-members had the same origins as those described for the deep waters of Emerald Basin and the central Scotian Shelf (Gatien 1976, Petrie & Drinkwater 1993, Houghton & Fairbanks 2001). Accordingly, the 3 end-members, described in terms of temperature (T , $^\circ\text{C}$), salinity (S , psu), and density (σ_t , kg m^{-3}), are hereafter referred to as Basin Water (BW, $T = 3$, $S = 32$, $\sigma_t = 25.5$), modified Basin Water (mBW, $T = 7$, $S = 33.3$, $\sigma_t = 26$), and intermediate Basin Water (iBW, $T = 4.8$, $S = 33.1$, $\sigma_t = 26.3$). The cold fresh BW originates in the GoSL and is advected along the inner Scotian Shelf by the NSCC. The mBW and iBW also originate in the GoSL, but the waters are advected along the continental slope by the outer arm of the NSCC, and as they are advected, they are modified as they mix with warmer and saltier slope waters. The iBW is colder, slightly fresher, and denser than mBW because it is modified by deeper slope waters.

End-member contributions in the deep Basin (100–160 m) varied horizontally both cross- and along-Basin (Fig. 2a). The eastern end of the Basin (Tr-1 to Tr-4 and eastern halves of Tr-9 and Tr-10) was a mixture of iBW and mBW. To the west (transition from blue to yellow; Fig. 2a), iBW was replaced by BW. From east to west, a transition from iBW to BW was particularly evident along Tr-8 and Tr-9 where all 3 end-members were encountered. The contribution of

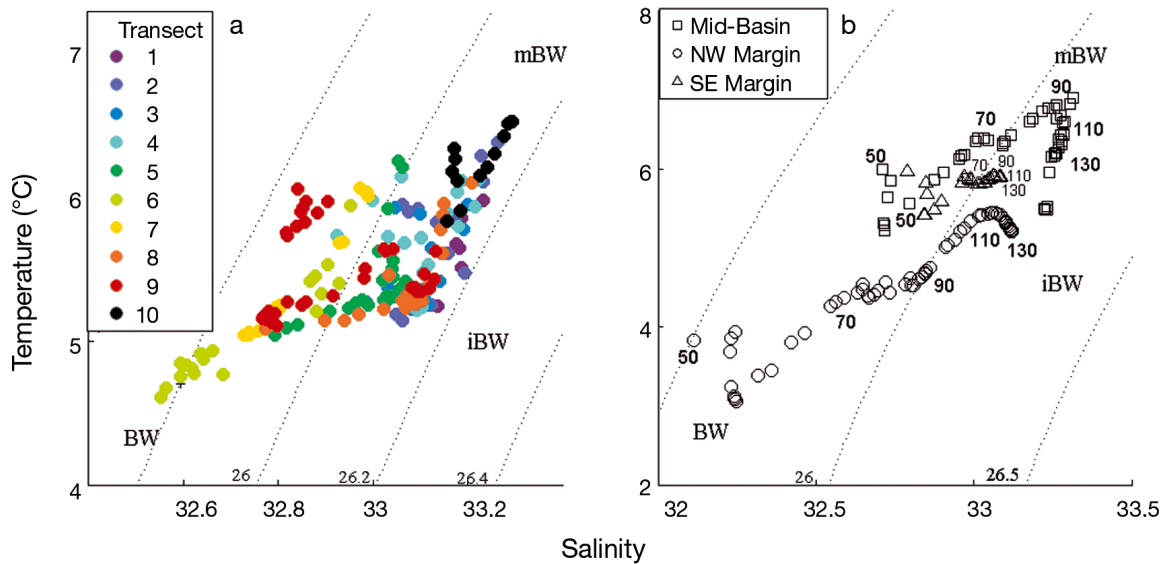


Fig. 2. Temperature–salinity (TS) diagrams with σ_t isopycnals (dotted lines, σ_t noted above abscissa) in Roseway Basin, September 2008, for (a) the deep-Basin water where each datum is the 100–160 m stratum-average along each color-coded transect (1 to 10, as in Fig. 1) with water mass end-members identified as Basin Water (BW), intermediate Basin Water (iBW), and modified Basin Water (mBW), and (b) 3 TS profiles from 50 m to the bottom of the tow (noted at beginning of each profile and at 20 m intervals) located at the NW margin (O), mid-Basin (□), and SE margin (Δ) of the Basin across Transect-2

each end-member also varied with depth, and the depth distribution of the water masses varied in a cross-Basin manner across the deepest part of the Basin (Tr-2). On the NW margin of Tr-2, BW dominated just below the thermocline at ~50 m, and its proportion decreased with increasing depth while the proportion of iBW increased (Fig. 2b). The mBW was absent on the NW margin. At mid-Basin along Tr-2, BW again dominated just below the thermocline, but it was warmer and saltier, indicating that it was mixed with mBW below it. The influence of BW decreased and mBW increased with increasing depth to ~100 m. Thereafter, mBW was replaced by iBW in the deepest part of the Basin. Near the SE margin, closest to the shelf break, the water was intermediate in its T–S signature between the NW margin and mid-Basin; this water was a mixture of all 3 water masses, with greater influence from the 2 slope-influenced waters than from BW (Fig. 2b). Spatial gradients in these end-members created significant variation in hydrography and strong water mass gradients throughout the Basin, discussed below.

Basin scale variation in water mass density

Sectional and planar distributions of T, S, and σ_t along all transects (Tr-1 to Tr-10) are provided in the Supplement (Figs. S8–S14), and we restrict our re-

sults here to water mass density as it is the most relevant to the diapausing calanoid copepods (Davies et al. 2013). Tr-2 and Tr-7 are representative of the density variation in the vertical and cross-isobath dimensions at the eastern and western Basin locations, respectively (Fig. 3a,b, see Fig. 1 for location). Cross-Basin tilting of the pycnocline upward toward the shelf break at depths above 100 m occurred at both the eastern and western margins of the Basin. Below 100 m on the SE margin, the isopycnals tilted downward toward the shelf break, indicating a transition to vertically well-mixed waters on the bank (Fig. 3a). To the west, where the bathymetry shoaled, density declined below $26 \sigma_t$ and the well mixed region on the SE margin disappeared (Fig. 3b). The planar distribution of density within the 100–160 m depth stratum showed that the highest-density water was located in the deep Basin near the NE margin, and a decreasing density gradient radiated outward in all directions (Fig. 4a–c). A particularly warm, high-salinity, and high-density water mass (i.e. ‘pure’ mBW) was located along the NE margin of the Basin (Fig. 4b,c) and illustrates the influence of the continental slope water. The depth distribution of the mBW mass, and its proximity to the shallow (relative to the Basin) channel separating Baccaro and Roseway banks (Fig. 1), indicates that this water entered the Basin from the continental slope through the channel.

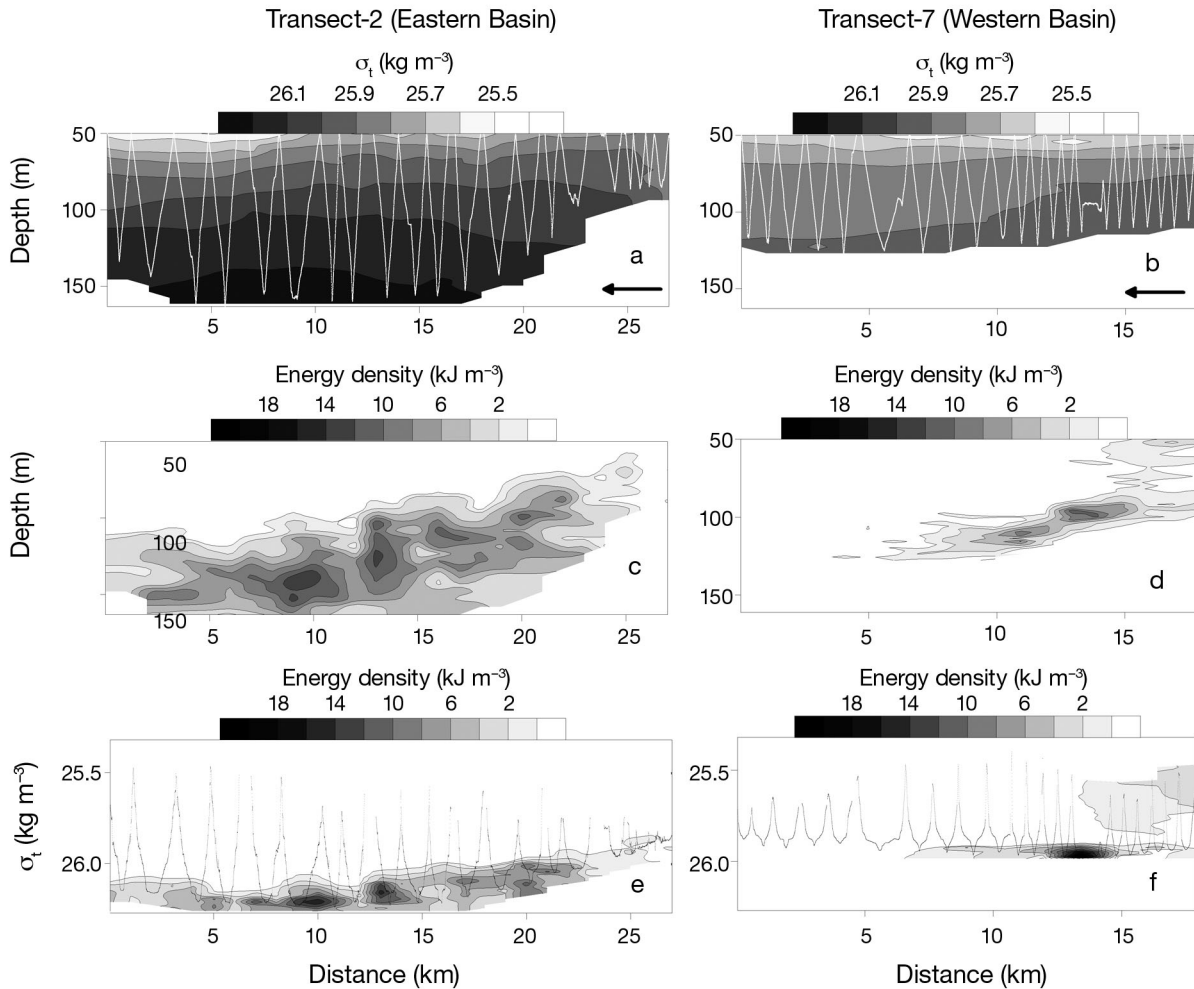


Fig. 3. Roseway Basin (a,b) water mass density (σ_t , kg m^{-3}) and (c,d) copepod energy density (kJ m^{-3}) at depth sections and (e,f) copepod energy density at σ_t sections in km from NW to SE along (a,c,e) Transect-2 in the eastern Basin and (b,d,f) Transect-7 in the western Basin where the arrows denote tow direction; vertically oscillating white lines in a and b and grey lines in e and f denote the tow profile, and blank regions at the bottom of each panel represent the seafloor

Basin scale variation in *Calanus* energy density

Comparisons made between sectional distributions of *Calanus* energy density and concentration (Fig. S4) demonstrate that the two are closely related; hence, inferences about the vertical positioning of *Calanus* can be drawn from estimates of energy density. Sectional distributions of *Calanus* energy density along all transects (Tr-1 to Tr-10) are provided in the Supplement (Figs. S5–S7). Analogous to the density sections, Tr-2 and Tr-7 are representative of the energy variation in the vertical and cross-isobath dimensions at the eastern and western Basin locations, respectively (Fig. 3c,d, see Fig. 1 for location). Along Tr-2, the energy density consistently increased with depth and by as much as an order of magnitude, reaching 2 kJ m^{-3} almost exclusively below 100 m

and with maximum densities near 12 kJ m^{-3} (Fig. 3c). The cross-Basin pattern also showed that the concentrated energy density spanned the width of the Basin and tilted upslope on the SE margin to a depth less than 100 m. At a smaller scale, high energy 'patches' spanning $\sim 1 \text{ km}$ in length and 1 to 10 m thick were distributed throughout the overall aggregation, and were particularly clustered in the deepest part of the Basin. To the west, energy density decreased and was only apparent along the shallower portion of the southern Basin margin along Tr-7 (Fig. 3d). The planar distribution of energy density showed that, consistent with the sectional profiles, the high energy aggregations were restricted to the deep Basin and were virtually absent on the western Basin margin (Fig. 4f,g). A 'tube' of high energy density extended along the Basin in a SW to NE direction in roughly

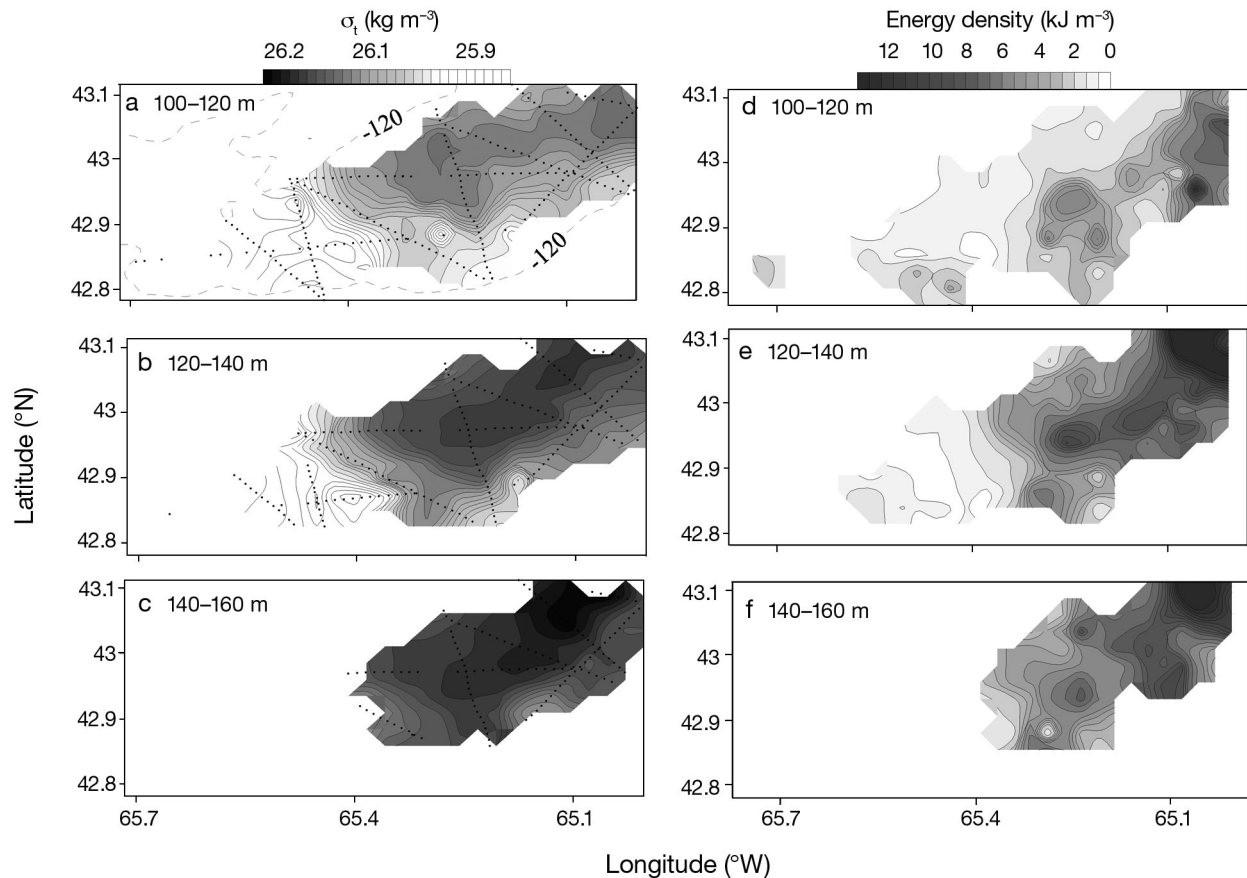


Fig. 4. Planar distribution of (a–c) depth-averaged water mass density (σ_t , kg m^{-3}) and (d–f) *Calanus* energy density (kJ m^{-3}) in September 2008 throughout Roseway Basin and within (a,d) the 100–120 m stratum, (b,e) the 120–140 m stratum, and (c,f) the 140–160 m stratum, where the 120 m isobath (dashed line) is provided in panel a and where each datum is indicated with black dots (a–c) along each of the transects illustrated in Fig. 1 (see the Supplement for all transect data)

the middle of the Basin, terminating in a large aggregation situated near the NE margin (Fig. 4d–f). The energy density within this tube was greatest in the 120–140 m depth layer (Fig. 4e), and its presence is entirely consistent with Davies et al. (2013), whose time series analysis estimated the length scale of the layer at 27 to 60 km.

***Calanus* energy density and hydrographic associations**

The distribution of the diapausing copepods in Roseway Basin reflected the influence of the slope water, particularly on mBW. Sectional distributions of energy density across Tr-2 and Tr-7, plotted as a function of water mass density (rather than depth), showed that across the entire Basin, the copepods were concentrated primarily at or below the 26 σ_t isopycnal (Fig. 3e,f). The slope-influenced water

masses (mBW and iBW) were both $\geq 26 \sigma_t$, while the water originating on the shelf (BW) was $< 26 \sigma_t$ (Fig. 2a). The highest energy densities were situated near the NE margin (Fig. 4e,f), where we hypothesized, based on the hydrography, that a slope-water intrusion was occurring (Fig. 4b,c). Virtually no copepods were present where the influence of BW was high along the northern and western margins, while a large aggregation was encompassed by the slope-water masses situated in the deep Basin and on the southern Basin margin (compare, for example, Fig. 4a with 4d). Finally, when the energy density estimates along each transect were examined in T–S space (Fig. 2a), it was apparent that the highest energy density in the Basin occurs where the influence of mBW was greatest (Fig. 5).

To examine more closely the energy density associations within the slope-influenced water masses, we compared energy density with water mass density below 100 m depth near the eastern Basin margin

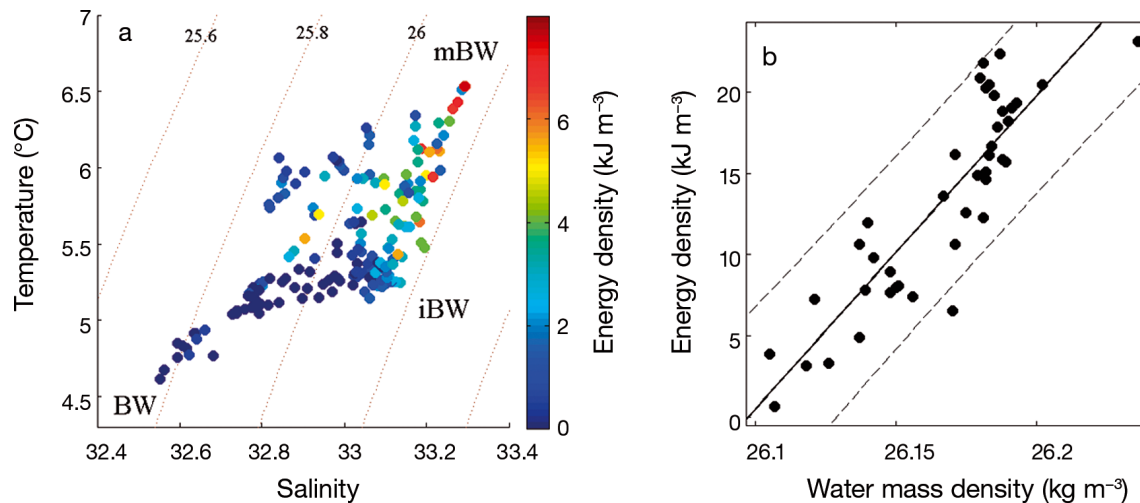


Fig. 5. (a) Depth averaged (100–160 m) diapausing copepod energy density (color-scaled kJ m^{-3}) in relation to depth averaged temperature and salinity (as in Fig. 2a), the isopycnals (dotted lines), and the Basin Water (BW), intermediate Basin Water (iBW), and modified Basin Water (mBW) end-member water masses. (b) Linear regression model (solid line) and 95% prediction interval (dashed lines) describe the increase in diapausing copepod energy density (kJ m^{-3}) as a function of water mass density (σ_t , kg m^{-3}) below 100 m depth on Transect-1 that was highly influenced by mBW

along Tr-1 where the slope-water intrusion was apparent (Fig. 4). This location was chosen because the slope water most resembles the mBW definition, and there was a strong ($r^2 = 0.82$) positive linear relationship between copepod energy density and water mass density (linear regression: energy density = $193\sigma_t - 5041$, $p < 0.001$, Fig. 5b). This too is consistent with Davies et al. (2013, their Fig. 10), who documented a very similar relation on the southern margin of the Basin. Above 100 m at that location, average energy density was negligible at $0.5 \pm 0.6 \text{ kJ m}^{-3}$.

When we examined copepod energy density as a function of depth, we observed cross-Basin tilting along the southern Basin margin (Fig. 3c,d). However, when energy density was examined as a function of water mass density, the prey field was less tilted, indicating that the cross-Basin isopycnal tilting is partially responsible for the phenomenon (Fig. 3e,f). The tilting of the prey field to shallower depths along the SE margin is a curious phenomenon that may be important for right whales given that the highest probability of observing a right whale occurs there (Fig. 9b and see Davies et al. 2013, Fig. 1), and this is specifically addressed below.

Tidal variation across the southern Basin margin

Variation in diapausing copepod energy density and water mass temperature was repeatedly (11 times) measured across a 12 to 15 km (tidal) transect that

straddled the southern margin of Roseway Basin (Fig. 6). However, water mass density was measured only during the first 2 transits (Fig. 7) due to operator error causing equipment failure. The first transit occurred during high tide, when the high temperature portion of the water mass was at its most downslope (deepest) location (Fig. 6g) and a $10 \text{ m} \times 4 \text{ km}$ aggregation of copepods, with an energy density of $\sim 15 \text{ kJ m}^{-3}$, was observed between the 2 and 6 km portion of the transect in the 120–140 m depth stratum (Fig. 6a). Energy density decreased upslope in the 6–15 km portion of the transit where, at the 8–12 km portion, the higher energy density was at a shallower depth and associated with the leading edge of a temperature gradient (Fig. 6g). On the Basin side of the gradient, the temperature was vertically stratified and the copepod aggregation was concentrated in the deeper homogeneous temperature layer. Downward tilting of the isopycnals near bottom at this location (Fig. 7e) demonstrated that the temperature gradient reflected a deep frontal region between stratified and well mixed waters. On the upslope side the water was less stratified, showing a strong horizontal gradient with warmer water on the bank. We use the above description to not only demonstrate the association between the water masses and energy density, but to demonstrate that we can use the thermal structure of the water to infer changes in water masses where we have no salinity and thus density estimates.

On the second and third transits, the front moved upslope with the ebbing tide (Fig. 6h,i), and the cope-

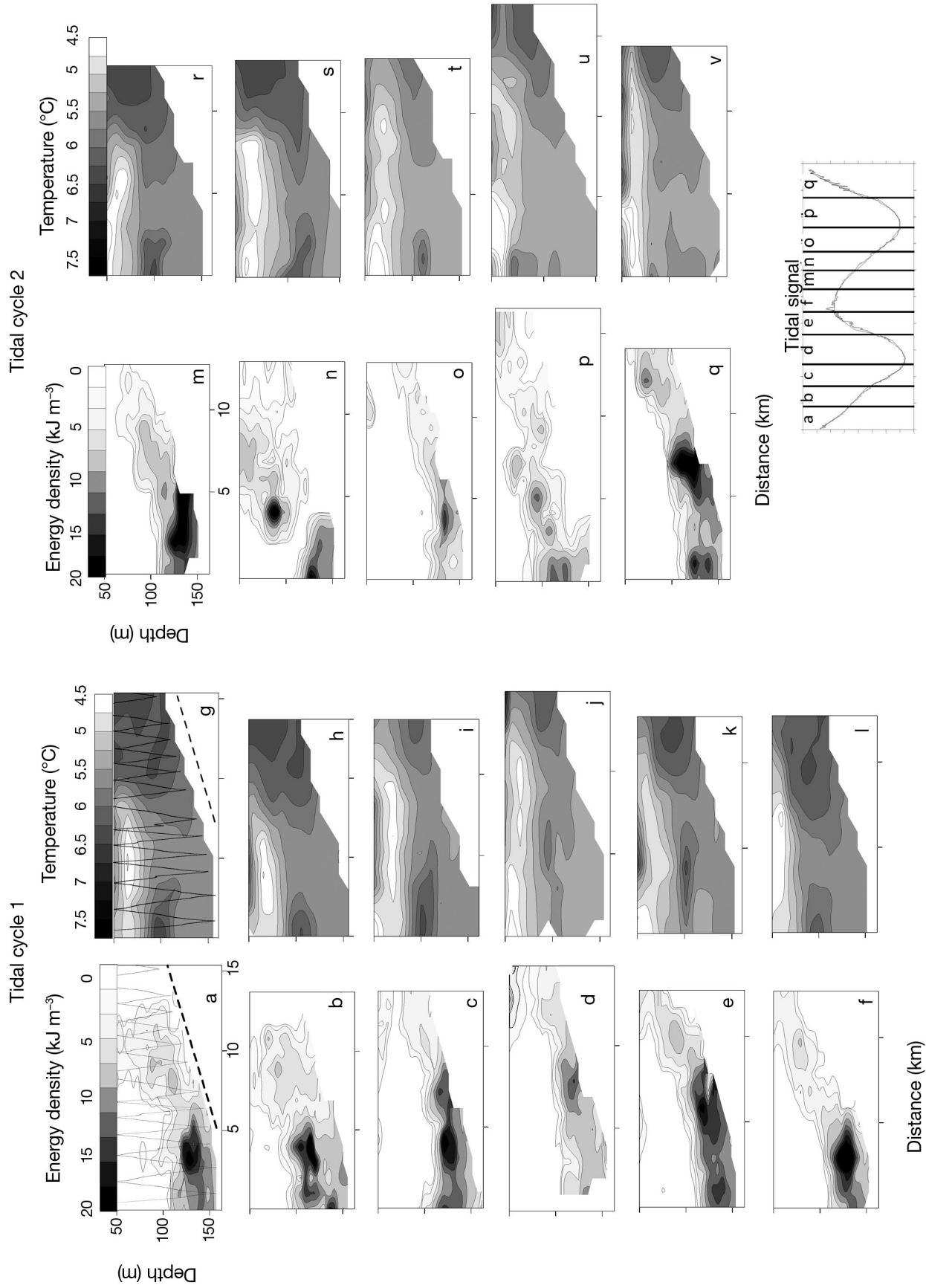


Fig. 6. (a–f, m–q) Diapausing copepod energy density (kJ m^{-3}) and (g–l, r–v) temperature ($^{\circ}\text{C}$) at depth sections over 2 tidal cycles (a–l and m–v) based on 11 transits over 24 h of the ~12 km cross-isobath tidal transect (see Fig. 1) straddling the southern margin of Roseway Basin. The stage of the tide during each transit is provided in the lower right panel. The approximate location of the seafloor is depicted by a dotted line in a and g and by the blank region in all other panels. Typical sampling profiles are shown by oscillating vertical grey and black lines in a and g, respectively

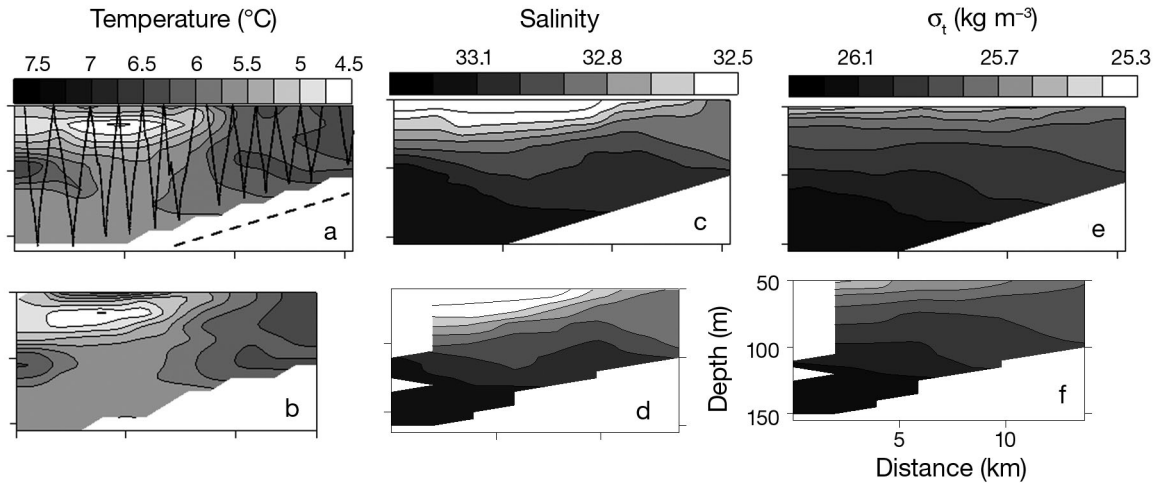


Fig. 7. (a,b) Temperature ($^{\circ}\text{C}$), (c,d) salinity, and (e,f) density (σ_t , kg m^{-3}) at depth sections along the first 2 of 11 transits (see Fig. 6a,b,g,h) of the ~ 12 km cross-isobath tidal transect (see Fig. 1) straddling the southern margin of Roseway Basin. The approximate location of the seafloor is depicted by a dotted line in panel a and by the blank region in all other panels. A typical sampling profile is provided in panel a

pod aggregation decreased as it spread upslope (Fig. 6b,c). At low tide, the aggregation almost disappeared, leaving a small near-bottom aggregation located ~ 8 km along the transect (Fig. 6d). The front was positioned on-bank near the 14 km location (Fig. 6d), and the water on the slope had a strong thermocline between 80 and 100 m depth that separated the cold upper water column from the warmer water and more dense water at depth. On the following flood tide, as the water and the front moved back downslope, the energy density aggregation reappeared and also moved downslope (Fig. 6e,f). During the second tidal cycle (Fig. 6m–v), the pattern was repeated in both the temperature and energy density sections. Once more this tidally driven upslope and downslope movement of the water masses and energy dense copepod aggregations are consistent with the time series of upslope and downslope excursions of highly concentrated copepods in the same region (see Fig. 9 in Davies et al. 2013), although we now have greater insight into the spatial extent of the energy-dense aggregations.

DISCUSSION

Summary

We have demonstrated that diapausing *Calanus finmarchicus* stage-C5 and *C. hyperboreus* stage-C4 copepods, primary prey for right whales in Roseway Basin, were concentrated below 100 m depth in large, high-energy aggregations that spanned the

deep Basin and tilted upslope on the southern Basin margin. Concentrations of these animals at depth varied spatially and over a tidal cycle with food energy density ranging from as low as near 0 to as high as $\sim 23 \text{ kJ m}^{-3}$. Large aggregations $>12 \text{ kJ m}^{-3}$ were particularly concentrated near the NE margin of the Basin below 120 m depth. Higher-frequency spatial and tidal variation in the prey energy field showed numerous smaller aggregations that were associated with particular water masses. Tidal variation near the southern margin indicated that the high-energy aggregates in the deep Basin were advected upslope as a water mass front moved upslope, and then reappeared on the opposite tide as the front moved downslope. Three water masses were defined in the deep water of Roseway Basin. The right whale prey were found primarily in the warmer, saltier slope-influenced water and were not found in the colder, fresher waters advected to the Basin from the GoSL by the inner arm of the NSCC. Within the slope-influenced water masses, copepod energy density was associated most often with mBW than iBW and was a strong and direct function of water mass density.

Mechanisms of prey aggregation

Davies et al. (2013) postulated that *Calanus* accumulated on the southern slope by being transported above their isopycnal of neutral buoyancy ($\sim 26 \text{ kg m}^{-3}$), then sinking back to this density layer, in a vertically sheared horizontal tidal current. If this mecha-

nism influenced copepod concentration, we expected to find energy density increasing on the downslope phase of the tide as the copepods returned to their depth of neutral buoyancy. We found that *Calanus* on the slope accumulated in large aggregations over the 2 tidal cycles that we measured; this is evidence that the mechanism we proposed appears to be acting on the Basin slope margin as it appears to do in the Grand Manan Basin (Michaud & Taggart 2011). Alternatively, the copepods could simply be vertically constrained by the near- $26 \sigma_t$ isopycnal. If so, the upslope and downslope movement of the density layer would result in vertical thickening and thinning on each tidal cycle over the Basin slope, and this may cause the copepod layer to disperse when the layer over the slope is thicker and then re-aggregate near-bottom when the layer thins.

The Basin-scale survey showed that the southern slope margin area of the Basin was not necessarily the only location where the highest energy density occurred; it was higher near the NE margin (Fig. 4d–f, and Fig. S1 in the Supplement). The southern margin was also where the prey field tilted upslope to shallower depths on the bank. Hence, right whales feeding on the slope could make shallower dives and find predictable, if smaller, energy-rich food aggregations than if they foraged in the deeper waters of the NE margin. This may explain why the probability of sighting a right whale is highest along the southern margin. There are, however, 2 caveats: (1) the aggregation we measured near the NE margin, which we hypothesize originates with a slope-water intrusion, may have been an episodic event and thus the energy density may not be consistently elevated in that region, or (2) the probability of observing right whales near the NE margin may not be well estimated (see below).

The diapausing copepods on the southern margin of Roseway Basin increase in concentration below the $26 \sigma_t$ isopycnal (Davies et al. 2013). Here we have shown that this pattern is consistent throughout the Basin. This association may have consequences for explaining variability in right whale habitat usage. For example, we found that the western Basin was devoid of *Calanus* in 2008, presumably because the water mass density was too low (Fig 4d–f). At other times, when water mass density is higher throughout the Basin, the suitable water-density habitat for the diapausing *Calanus*, and thus the whales, would be expanded toward the western margin. Further, during times when water mass density is higher throughout the Basin than we observed, copepods residing along the margins would accumulate below

the isopycnal farther upslope, which would provide metabolic benefit to a diving whale (Fig. 8). The opposite would occur during times when water mass density throughout most of the Basin was lower than we observed (Fig. 8). The above arguments offer a plausible mechanism that could explain the apparent inter-annual relationship between right whales, copepods, and water mass density in Roseway Basin as suggested by Patrician & Kenney (2010). Next, we discuss how *Calanus* associations with particular source water masses that vary in density may facilitate such a mechanism.

Calanus source water advection into Roseway Basin

The relative contributions from different Scotian Shelf copepod sources to Roseway Basin depend on production and advection from upstream at the surface in winter, spring, and summer (Tremblay & Roff 1983, Herman et al. 1991, Head et al. 1999, Zakard-

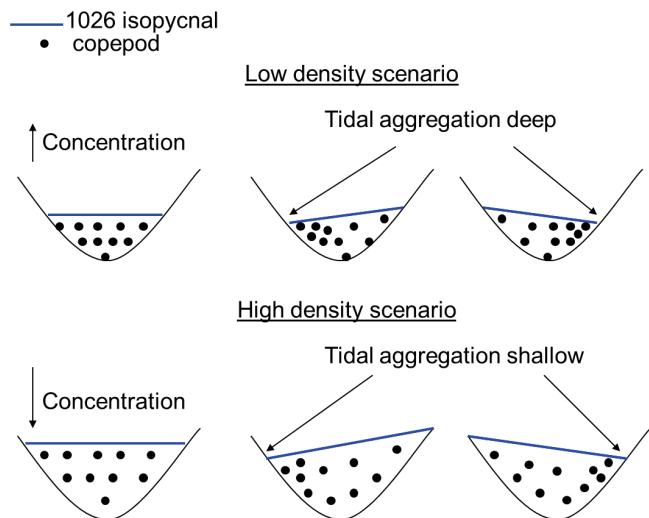


Fig. 8. Alternative scenarios in which the mechanistic relationship between water mass density and diapausing copepod aggregation in a basin influence right whale foraging, assuming the diapausing copepod abundance is the same under both scenarios. In the low-density scenario, the 1026 kg m^{-3} isopycnal resides deep, and the copepods aggregate in high concentrations near the bottom. As the isopycnal moves up and down at the basin margins, the aggregation of copepods at the margin occurs deep. In the high-density scenario, the 1026 kg m^{-3} isopycnal resides shallow, and the copepods are lower in concentration because they are not as vertically restricted. As the isopycnal moves up and down at the basin margin, that aggregation of copepods at the margin occurs upslope and closer to the bank than in the low-density scenario

jian et al. 2003). All Shelf sources, e.g. other Shelf basins and subsequent Shelf production, the GoSL outflow, and slope-water intrusions at the surface in spring, contribute to the diapausing copepod population in Roseway Basin, and our measurements in late summer in the western-most Shelf Basin were the result of many processes. We were able to observe the influence of at least 1 source. The presence of slope-influenced water, containing the highest *Calanus* energy density near the entrance of the channel connecting Roseway Basin to the continental slope, allows us to infer that intrusions from the continental slope through the deep channel in summer may provide substantial concentrations of diapausing copepods to the Basin.

The absence of copepods in cold, fresh BW located in the western end of the Basin could occur for several reasons. One is that BW is not sufficiently dense to retain diapausers, and copepods entering diapause in the BW either sink to the seafloor or are swept into the deep Basin, which is filled with higher density slope-influenced water. The other is that the Shelf was not a significant source of copepods to Roseway Basin in 2008. Zooplankton biomass on the eastern Scotian Shelf, upstream of Roseway Basin in March, was near the lowest on record (Harrison et al. 2009). Zooplankton biomass and *Calanus finmarchicus* abundance were each anomalously low in May, and each exhibited late maxima (June to August relative to the April to June norm) of near-average magnitude offshore of Halifax, Nova Scotia. The maximum concentration of *C. finmarchicus* in June to August was normal at $60\,000\text{ m}^{-2}$, but 70% lower than the spring maximum in 2007.

Interannual variation in *Calanus* abundance at depth in Roseway Basin has been hypothesized to explain the absence of right whales in some years (Patrician & Kenney 2010). Processes that affect water mass density at depth in the Basin, for example by increased volume transport of BW or variation in the frequency and strength of slope-water intrusions, could also affect the copepod concentrations in the Basin by varying the density of the deeper waters, e.g. if the water becomes so low in density that the copepods either sink out of the water column or cease diapause and molt to adults. If, as we propose, summer intrusions of deep slope water are an important source of copepods to Shelf basins, variation in the frequency and strength of slope intrusions would have a significant impact in Roseway Basin independent of the density variation in the Basin, thus driving the mechanism proposed in Fig. 8.

CH definition for Roseway Basin and evaluation of provisional CH boundaries

Based on the above results, CH in Roseway Basin can now be refined as the area that contains high energy density of right whale food, i.e. co-located with diapausing *Calanus finmarchicus* stage-C5 and *C. hyperboreus* stage-C4. The refinement is based on the oceanographic and bathymetric conditions that promote aggregation of the copepods at depths >100 m in waters that are influenced by off-Shelf water (particularly mBW), with which the copepods are associated. During the period of maximum seasonal occupancy of right whales in Roseway Basin (August to September), the highest food energy density was situated along the southern slope margin and particularly in the eastern half of the provisional CH (Fig. 9a). The eastern portion of the Basin is where the influence of the high-density mBW was most apparent. It is clear that bathymetric depth and water mass density are 2 of the most important and easily identifiable oceanographic conditions related to large aggregations of energy-rich right whale food that can be used to refine the CH boundaries.

We determined that the boundaries of the 'static' high energy-density field was encompassed, at a minimum, by the 120 m isobath and thus within the provisional CH boundary (Fig. 9a). Ignoring any average residual current, the movement of the planktonic prey field is ~3 km over a tidal cycle, and the cross-isobath tidal ellipse transports the prey field across the southern Basin margin between the 100 and 140 m isobaths (Davies et al. 2013), implying that the provisional boundaries are sufficient to envelope the entire habitat as it moves over tidal and diel scales. Although we did not measure high energy density or the appropriate oceanographic conditions associated with high energy density in the western half of the provisional CH in 2008, we speculate that the western margin may be used frequently as a feeding habitat in other years when the 1026 isopycnal is located higher in the water column in the Basin. We explore this issue in a subsequent manuscript. In summary, it appears that the provisional northern, southern, and western CH boundaries are appropriate — but what of the eastern boundary?

At the eastern margin of Roseway Basin, where the channel joins the Basin, we encountered a warm, salty, and high-density water mass that contained a large aggregation of diapausing copepods, the largest and highest energy-density aggregation measured in the Basin. Our survey design did not extend into the channel corridor as we were unaware

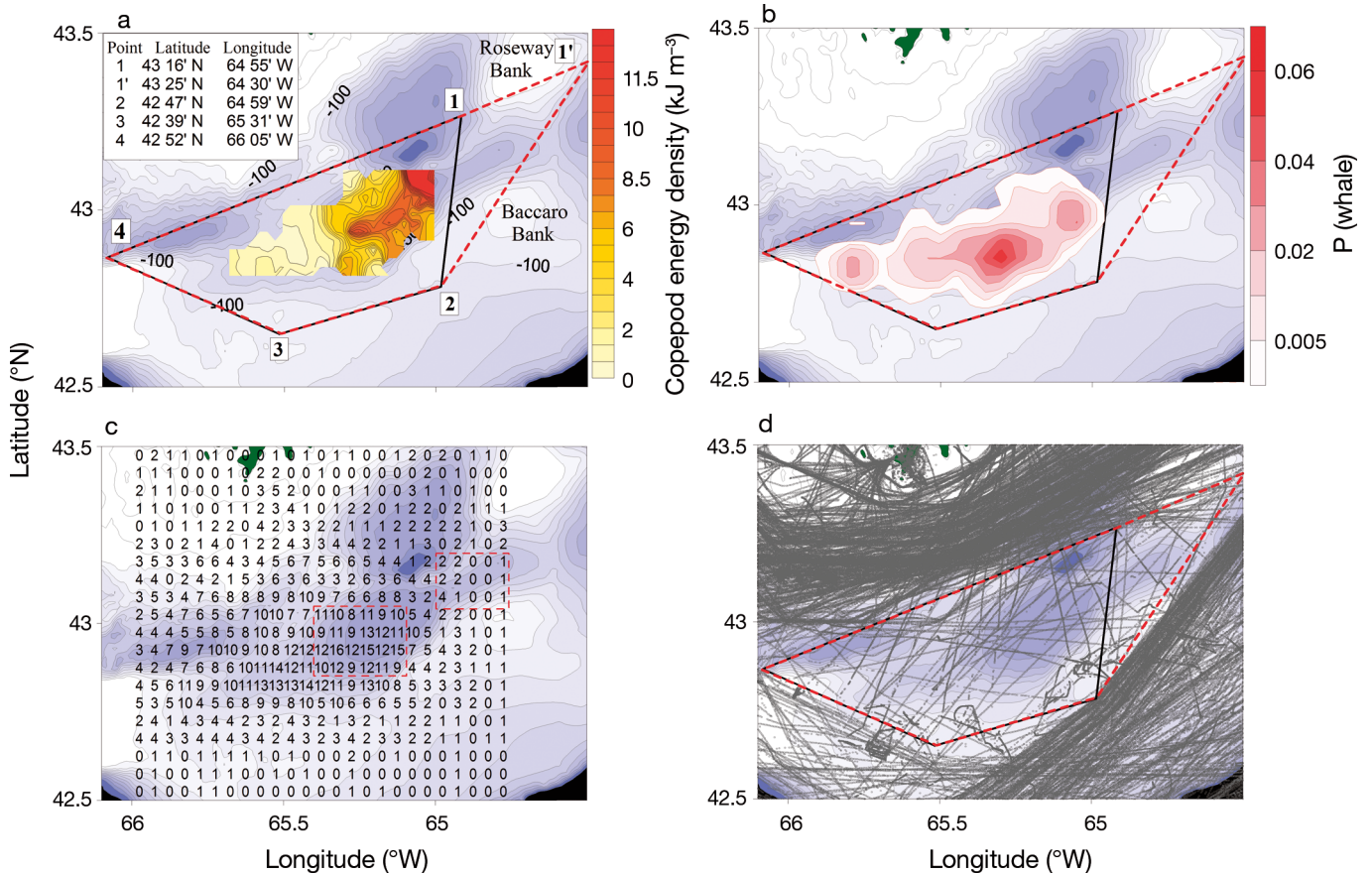


Fig. 9. Bathymetric chart (10 m intervals) of the distribution of (a) copepod energy density (kJ m^{-3}) in the 140–160 m depth stratum in the Roseway Basin Critical Habitat (CH). The recommended extension of the CH boundaries is compared with (b) the relative probability of observing a right whale (P [whale]) in the Roseway Basin CH (NARWC 2008), (c) the number of years each grid cell in the Roseway Basin study area has been surveyed for right whales, where the red rectangles compare regions of high and low survey effort referred to in the text, and (d) vessel tracks (grey lines) through the CH after the voluntary Area to be Avoided (ATBA) was implemented (from Vanderlaan & Taggart 2009). The CH boundaries are shown in black in panels a, b, and d, the recommended extension is the dotted red line in a, b, and d, and the geographic positions of the CH corners are provided in panel a

of its potential importance at the time because the survey design was based primarily on the right whale probability distribution. Although we have reasonably strong evidence, based on the water mass characteristic and the energy density, that the channel between Roseway and Baccaro banks conforms to the above definition of CH, it does not appear to conform to the right whale probability distribution. To address why this may be, we examined the veracity of the right whale probability distribution. An area encompassing 15 survey grid cells (used in estimating historical right whale probability distribution) that is located near or within the 100 m isobath and extends into the channel, is located due east of our survey coverage (Fig. 9c). On average, each grid cell has been surveyed 1.1 times in 20 yr (105% coefficient of variation). Conversely, the area encompassing 24 survey grid cells near or within the core of the

whale probability distribution (Fig. 9c) has been surveyed on average 11.2 times in 20 yr (18% coefficient of variation). Thus, the probability of observing a right whale near the eastern margins of the Basin is extremely uncertain, i.e. it is impossible to determine whether right whales use the corridor regularly due to extremely low sampling effort. Thus, based on the precautionary principle, and on the above information concerning oceanographic indicators of CH with respect to SARA and the Recovery Strategy, we recommend that the eastern boundary of the provisional CH be refined to include what appears to be an ecologically important area. This could be achieved by extending the NE apex of the provisional CH boundary from location 1 to location 1' (Fig. 9a). While our recommendation is based on a single year of data, we will explore the interannual variation in CH in a subsequent manuscript.

The provisional CH boundaries were designed to conform with the voluntary Area to be Avoided (ATBA) boundaries adopted by Canada and the International Maritime Organization (IMO) in 2008 (Vanderlaan & Taggart 2009), and the ATBA was designed to encompass the probability distribution of right whales (Vanderlaan et al. 2008), making it the most important conservation measure for the Roseway Basin CH. Before the ATBA implementation, vessels transited directly through the Basin. After implementation, most vessels voluntarily navigated around the ATBA (Vanderlaan & Taggart 2009, Fig. 9d). The provisional CH boundaries could be modified to protect the northeast corridor into the Basin simply by modifying the ATBA. Such a refinement would come at virtually no cost to mariners because it is abundantly clear that the majority of vessels already voluntarily re-route around the corridor (Fig. 9d). Refinement of the ATBA can easily be achieved as there is precedence, viz. the IMO refinement of the port of Boston (Massachusetts, USA) traffic separation scheme (Silber et al. 2012).

CONCLUSIONS

We achieved our ultimate goal of refining the right whale CH in Roseway Basin by defining and identifying the CH for right whales based on their prey field distribution and the processes that aggregate the copepod food base in the Basin. Further, high resolution co-located copepod and hydrographic sampling allowed us to meet our secondary objectives concerning the sources, retention, and accumulation of the copepods within the habitat. Oceanographic processes that affect the energy density field in Roseway Basin include slope-water intrusions and the water mass density field. This is also the first large-scale oceanographic survey of Roseway Basin, and hence advances general knowledge of the biological and physical oceanography on the Scotian Shelf.

This is part of a series of precedent-setting studies in marine conservation because the North Atlantic right whale is the first marine species in Canada for which the biological and physical components of CH have been characterized robustly and at multiple scales. CH, in both the Grand Manan and Roseway Basins, is already aligned with effective conservation policies that protect whales from lethal vessel strikes, and options for enhanced habitat protection from fishing gear entanglements are ready for policy consideration (e.g. Vanderlaan et al. 2011).

Acknowledgements. We thank D. Brownell, M. Hatcher, W. Judge, D. Schillinger, A. Vanderlaan, and the crew of the RV 'Dominion Victory' for help with field work, and P. Aven-dano, M. Morgan, J. Slade, and A. Ryan for sample processing. We thank M. Baumgartner, B. Petrie, Y. Simard, K. Thompson, and T. Ross for valuable insights and suggestions and A. Vanderlaan for providing Fig. 9d. Funding for this research was provided to C.T.T. by the Fisheries and Oceans Canada Species at Risk Program (DFO SARP), the Environment Canada (EC) – WWF Endangered Species Fund, the EC Habitat Stewardship Program, and a Natural Sciences and Engineering Research Council (NSERC) Discovery Grant. Additional funding was provided to R.K.S. by the EC Interdepartmental Recovery Fund for Species at Risk and DFO SARP. K.T.A.D. was supported by an NSERC PSG-M Scholarship.

LITERATURE CITED

- Baumgartner MF, Mate BR (2003) Summertime foraging ecology of North Atlantic right whales. *Mar Ecol Prog Ser* 264:123–135
- Baumgartner MF, Mate BR (2005) Summer and fall habitat of North Atlantic right whales (*Eubalaena glacialis*) inferred from satellite telemetry. *Can J Fish Aquat Sci* 62: 527–543
- Baumgartner MF, Cole TVN, Clapham PJ, Mate BR (2003a) North Atlantic right whale habitat in the lower Bay of Fundy and on the SW Scotian Shelf during 1999–2001. *Mar Ecol Prog Ser* 264:137–154
- Baumgartner MF, Cole TVN, Campbell RG, Teegarden GJ, Durbin EG (2003b) Associations between North Atlantic right whales and their prey, *Calanus finmarchicus*, over diel and tidal time scales. *Mar Ecol Prog Ser* 264:155–166
- Baumgartner MF, Mayo CA, Kenney RD (2007) Enormous carnivores, microscopic food and a restaurant that's hard to find. In: Krauss SD, Rolland R (eds) *The urban whale: North Atlantic right whales at the crossroads*. Harvard University Press, Cambridge, MA, p 138–171
- Brown MW, Fenton D, Smedbol K, Merriman C, Robichaud-Leblanc K, Conway JD (2009) Recovery Strategy for the North Atlantic Right Whale (*Eubalaena glacialis*) in Atlantic Canadian Waters. Species at Risk Act Recovery Strategy Series. Fisheries and Oceans Canada, Ottawa, ON
- Davies KTA, Ryan A, Taggart CT (2012) Measured and inferred gross energy content in diapausing *Calanus* spp. in a Scotian Shelf basin. *J Plankton Res* 34:614–625
- Davies KTA, Ross T, Taggart CT (2013) Tidal and subtidal currents affect deep aggregations of right whale prey, *Calanus* spp., along a shelf-basin margin. *Mar Ecol Prog Ser* 479:263–282
- Fleminger AH, Hulsemann K (1977) Geographical range and taxonomic divergence in North Atlantic *Calanus* (*C. helgolandicus*, *C. finmarchicus* and *C. glacialis*). *Mar Biol* 40:233–248
- Gatien MG (1976) A study in the slope water region south of Halifax. *J Fish Res Board Can* 33:2213–2217
- Han G, Hannah CG, Loder JW, Smith PC (1997) Seasonal variation of the three-dimensional mean circulation over the Scotian Shelf. *J Geophys Res* 102:1011–1025
- Hannah CG, Shore JA, Loder JW, Naimie CE (2001) Seasonal circulation on the western and central Scotian Shelf. *J Phys Oceanogr* 31:591–615

- Harrison G, Johnson C, Head E, Spry J and others (2009) Optical, chemical, and biological oceanographic conditions in the Maritimes Region in 2008. DFO CSAS Res Doc 2009/054. Available at <http://www.dfo-mpo.gc.ca/csas/>
- Head EJH, Harris LR, Petrie B (1999) Distribution of *Calanus* spp. on and around the Nova Scotia shelf in April: evidence for an offshore source of *Calanus finmarchicus* to the central and western regions. *Can J Fish Aquat Sci* 56: 2463–2476
- Herman AW (1988) Simultaneous measurement of zooplankton and light attenuation with a new optical plankton counter. *Cont Shelf Res* 8:205–221
- Herman AW (1992) Design and calibration of a new optical plankton counter capable of sizing small zooplankton. *Deep-Sea Res* 39:395–415
- Herman AW, Sameoto DD, Shunian C, Mitchell MR, Petrie B, Cochrane N (1991) Sources of zooplankton on the Nova Scotia shelf and their aggregation within deep basins. *Cont Shelf Res* 11:211–238
- Houghton RW, Fairbanks RG (2001) Water sources for Georges Bank. *Deep-Sea Res II* 48:95–114
- Kenney RD, Hyman MAM, Owen RE, Scott GP, Winn HE (1986) Estimation of prey densities required by North Atlantic right whales. *Mar Mamm Sci* 2:1–13
- Kenney RD, Mayo CA, Winn HE (2001) Migration and foraging strategies at varying spatial scales in western North Atlantic right whales: a review of hypotheses. *J Cetacean Res Manag 2(Spec Issue)*:251–260
- Kraus SD, Rolland RM (2007) Right whales in the urban ocean. In: Kraus SD, Rolland R (eds) *The urban whale: North Atlantic right whales at the crossroads*. Harvard University Press, Cambridge, MA, p 1–38
- McLaren IA, Head E, Sameoto DD (2001) Life cycles and seasonal distributions of *Calanus finmarchicus* on the central Scotian Shelf. *Can J Fish Aquat Sci* 58:659–670
- Michaud J, Taggart CT (2007) Lipid and gross energy content of North Atlantic right whale food, *Calanus finmarchicus*, in the Bay of Fundy. *Endang Species Res* 3:77–94
- Michaud J, Taggart CT (2011) Spatial variation in right whale food, *Calanus finmarchicus*, in the Bay of Fundy. *Endang Species Res* 15:179–194
- Murison LD, Gaskin DE (1989) The distribution of right whales and zooplankton in the Bay of Fundy, Canada. *Can J Zool* 67:1411–1420
- NARWC (North Atlantic Right Whale Consortium) (2008) North Atlantic Right Whale Consortium sightings database, 22 July 2008. New England Aquarium, Boston, MA
- Patrician MR, Kenney RD (2010) Using the continuous plankton recorder to investigate the absence of North Atlantic right whales (*Eubalaena glacialis*) from the Roseway Basin. *J Plankton Res* 32:1685–1695
- Petrie B, Drinkwater K (1993) Temperature and salinity variability on the Scotian Shelf and in the Gulf of Maine 1945–1990. *J Geophys Res* 98:20079–20089
- Planque B, Batten SD (2000) *Calanus finmarchicus* in the North Atlantic: the year of *Calanus* in the context of interdecadal change. *ICES J Mar Sci* 57:1528–1535
- Sameoto DD, Herman AW (1990) Life cycle and distribution of *Calanus finmarchicus* in deep basins on the Nova Scotia shelf and seasonal changes in *Calanus* spp. *Mar Ecol Prog Ser* 66:225–237
- Sameoto DD, Jaroszynski LO, Fraser WB (1980) BIONESS, a new design in multiple net zooplankton samplers. *Can J Fish Aquat Sci* 37:722–724
- Silber GK, Vanderlaan ASM, Tejedor Arceredillo A, Johnson L and others (2012) The role of the International Maritime Organization in reducing vessel threat to whales: process, options, action and effectiveness. *Mar Policy* 36: 1221–1233
- Sprules WG, Jin EH, Herman AW, Stockwell JD (1998) Calibration of an optical plankton counter for use in fresh water. *Limnol Oceanogr* 43:726–733
- Taggart CT, Thompson K, Maillet G, Lochmann S, Griffin D (1996) Abundance distribution of larval cod (*Gadus morhua*) and zooplankton in a gyre-like water mass on the Scotian Shelf. In: Watanabe Y, Yamashita Y, Oozeki Y (eds) *Survival strategies in early life stages of marine resources*. Proceedings of the International Workshop, Yokohama. Balkema Press, Rotterdam, p 155–173
- Tremblay MJ, Roff JC (1983) Community gradients in the Scotian Shelf zooplankton. *Can J Fish Aquat Sci* 40: 598–611
- Vanderlaan ASM (2010) Estimating the risk to the North Atlantic right whale (*Eubalaena glacialis*) from ocean-going vessels and fishing gear. PhD dissertation, Dalhousie University, Halifax, NS
- Vanderlaan ASM, Taggart CT (2009) Efficacy of a voluntary area to be avoided to reduce risk of lethal vessel strikes to endangered whales. *Conserv Biol* 23:1467–1474
- Vanderlaan ASM, Taggart CT, Serdynska AR, Kenney RD, Brown MW (2008) Reducing the risk of lethal encounters: vessels and right whales in the Bay of Fundy and on the Scotian Shelf. *Endang Species Res* 4:283–297
- Vanderlaan ASM, Taggart CT, Smedbol RK (2011) Fishing-gear threat to right whales (*Eubalaena glacialis*) in Canadian waters and the risk of lethal entanglement. *Can J Fish Aquat Sci* 68:2174–2193
- Woodley TH, Gaskin DE (1996) Environmental characteristics of North Atlantic right and fin whale habitat in the lower Bay of Fundy, Canada. *Can J Zool* 74:75–84
- Zakardjian BA, Sheng J, Runge JA, McLaren IA, Plourde S, Thompson KR, Gratton Y (2003) Effects of temperature and circulation on the population dynamics of *Calanus finmarchicus* in the Gulf of St. Lawrence and Scotian Shelf: study with a coupled three-dimensional hydrodynamic, stage-based life history model. *J Geophys Res* 108, 8016, doi:10.1029/2002JC001410

Editorial responsibility: Peter Corkeron,
Woods Hole, Massachusetts, USA

Submitted: May 10, 2013; Accepted: October 7, 2013
Proofs received from author(s): December 26, 2013